

# Artesunate disrupts germ layer formation by inhibiting BMP signaling pathway

Myeoung Su Kim <sup>\*</sup>, Gang-Ho Yoon <sup>\*</sup> and Sun-Cheol Choi 

Department of Biochemistry and Molecular Biology, Brain Korea 21 Project, University of Ulsan College of Medicine, Asan Medical Center, Seoul, Korea

## ABSTRACT

*Xenopus* embryo is a useful model for evaluating the adverse effects of any compounds on the cellular processes essential for early development and adult tissue homeostasis. Our chemical library screening with frog embryos identified artesunate (ART) as an inhibitor of the BMP signaling pathway to interfere with the specification of embryonic germ layers. Exposure to ART led to reduction of the anterior-posterior body axis, malformed tail structures and loss of pigment cells in the trunk region of embryos. The severely defective embryos exhibited truncation of posterior structures, resembling the phenotypes of tadpoles depleted of BMPs. Consistent with these morphological deformities, ART exposure inhibited the BMP-dependent transcriptions of target genes and specification of ventral mesoderm. In contrast, the expression of an organizer-specific gene induced by Activin/Nodal signaling remained unchanged in ART-treated cells. ART also enhanced anterior neural differentiation at the expense of epidermal and neural crest cell fates. Unexpectedly, we observed that ART exposure accelerates proteasomal degradation of a BMP transducer Smad1, leading to upregulation of MAP kinase activity. Taken together, these results suggest that ART acts as an inhibitor of BMP signaling pathway, exerting severe adverse effects on the specification of germ layers in vertebrate early development.

## ARTICLE HISTORY

Received 7 April 2025  
Revised 23 April 2025  
Accepted 6 May 2025

## KEYWORDS


Artesunate; BMP signaling;  
MAPK; Teratogenicity;  
*Xenopus*

## Introduction


In the *Xenopus* early embryo, the mesodermal cell fate is induced in the marginal zone between the animal and vegetal poles at the mid-blastula stage by a dorsal-ventral gradient of several Nodal-related signals from the underlying endoderm (De Robertis et al. 2000). Low levels of Nodal signals result in the formation of ventral mesoderm, whereas high levels lead to the establishment of Spemann's organizer in the dorsal mesoderm. At the gastrula stage, bone morphogenetic protein (BMP) inhibition by the antagonists emanating from the organizer, such as Chordin and Noggin, generates a ventral-to-dorsal gradient of BMP activity, refining the initial patterning of the mesodermal layer (De Robertis and Kuroda 2004). These BMP inhibitors are secreted molecules that bind to BMPs directly in the extracellular space, preventing them from binding to and signaling through their cognate receptors. In the mesoderm of *Xenopus*, no BMP is required for notochord formation, low BMP for myogenic differentiation and high BMP for blood development (Niehrs 2004). In the ectoderm,

epidermal differentiation occurs in the presence of high BMP signals, whereas neural tissues are formed when the BMP antagonists inhibit BMP signaling. Thus, the antagonism between BMPs and their inhibitors plays critical roles in the patterning of the embryonic germ layers.

BMPs, a subset of the TGF- $\beta$  superfamily of cytokines, regulate many aspects of vertebrate development including patterning of the limb and somites, bone formation and organogenesis (Hogan 1996; Zhao 2003). These proteins exert their effects through cell-surface serine-threonine kinase receptors, designated type I and type II (BMPRI and BMPRII). Upon ligand binding, constitutively active type II receptors phosphorylate type I receptors, propagating the signal by phosphorylating receptor regulated Smads (R-Smads), Smad1/5/8 at their distal C-termini. These phosphorylated BMP-specific Smads form a complex with the co-Smad, Smad4, and translocate into the nucleus. In the nucleus, the R-Smad/Smad4 complex controls the transcription of BMP-responsive genes by binding to their

**CONTACT** Sun-Cheol Choi  choisc@amc.seoul.kr 

\*These authors equally contributed to this work.

 Supplemental data for this article can be accessed online at <https://doi.org/10.1080/19768354.2025.2504940>.

© 2025 The Author(s). Published by Informa UK Limited, trading as Taylor & Francis Group

This is an Open Access article distributed under the terms of the Creative Commons Attribution-NonCommercial License (<http://creativecommons.org/licenses/by-nc/4.0/>), which permits unrestricted non-commercial use, distribution, and reproduction in any medium, provided the original work is properly cited. The terms on which this article has been published allow the posting of the Accepted Manuscript in a repository by the author(s) or with their consent.

promoters with cofactors such as OAZ and STAT3 (Moustakas and Heldin 2009; Wu and Hill 2009).

BMP signaling is integrated with other signaling pathways in achieving specific cell differentiation during early development. BMP-4 and FGF signals cooperates with each other in inducing paraxial mesoderm specification (Kumar et al. 2024). The FGF/MAPK pathway has been shown to induce an inhibitory phosphorylation in the linker region of BMP transducer Smad1 at conserved MAPK sites (Pera et al. 2003; Sapkota et al. 2007). This linker phosphorylation by MAPK serves as priming for subsequent phosphorylation at GSK3 sites located near the MAPK sites, leading to Smurf1-mediated polyubiquitination and proteasome-dependent degradation of Smad1 (Fuentealba et al. 2007). Thus, FGF signaling opposes the effect of Smad1 phosphorylation at C-terminal sites by BMP receptor, thereby promoting neural development at the expense of epidermal cell fates. Furthermore, Wnt signaling down-regulates GSK3 activity, contributing to the stabilization of BMP-activated Smad1 and the prolonged duration of BMP signals. Hence, Wnt signaling induces epidermis in a Smad1-dependent manner.

Artesunate (ART), mainly known as an anti-malarial drug, is a semisynthetic derivative of artemisinin, the bioactive component isolated from the Chinese medicinal herb called *Artemisia annua* (Yang et al. 2021; Gong et al. 2022). Accumulating evidence has shown that ART also has broad anti-cancer effects on various tumor cells (Chen et al. 2021; Cao et al. 2022). For instance, ART has been shown to induce apoptosis, necrosis, and autophagy in human cancer cells. The anti-tumor properties of ART also include the following mechanisms: cell cycle arrest, reduction of cell invasion and metastasis, production of reactive oxygen species (ROS), inhibition of angiogenesis, and ferroptosis. Although ART-mediated cell death and its therapeutic efficacy have been studied in detail, its effects on the early development of vertebrates remain largely unknown.

*Xenopus* has been a useful model for studying various cellular processes, such as gene regulatory network and DNA damage responses (Goutam et al. 2024; Kim et al. 2024), and for assessing the teratogenicity of chemicals (Park et al. 2016). In this study, screening of a chemical library has been performed to identify natural compounds that exhibit specific effects on key signaling pathways in early development. To this end, *Xenopus* embryos were treated with each chemical from the one-cell to tadpole stages, and the resulting morphological deformities were observed. In this screening, ART was found to exert disruptive effects on the patterning of dorsoventral body axis of embryo. Thus, ART-exposed embryos showed defective specification of ventral mesoderm, and expansion of anterior type of

neural tissue at the expense of epidermal cell fate. Of note, these effects of ART were achieved by inducing Smad1 degradation, which leads to down-regulation of BMP signaling. Together, these results suggest that ART exposure causes severe teratogenicity by targeting specifically BMP signaling pathway.

## Materials and methods

### *In vitro* fertilization and embryo manipulation

Male and female *Xenopus laevis* frogs were purchased from Korean *Xenopus* Resource Center for Research. Unfertilized eggs from *Xenopus laevis* primed with 500 units of human chorionic gonadotropin (HCG, Deasung Microbiological Labs.) were *in vitro* fertilized using macerated testis, dejellied in 2% cysteine solution (pH 7.8) and cultured in 0.33 × Modified Ringer (MR) until stage 8 and then transferred to 0.1 × MR with gentamicin (Gibco, 15710072). The developmental stages of the embryos were determined according to the normal table of *Xenopus* development described in (Zahn et al. 2022). For animal cap assays, animal cap explants were excised at stage 8.5 from whole embryos, cultured to the denoted stages in 1 × MR containing bovine serum albumin (BSA, 10 µg/ml; Roche, 10735086001) and gentamicin (50 µg/ml) and then subjected to further experiments.

### mRNA synthesis, constructs and chemicals

Capped mRNAs were *in vitro* synthesized by using a mMessage mMachine kit (Ambion, Austin, TX) and linearized DNA as a template. The following constructs were described previously: *DN FGFR1* (Ribisi et al. 2000); *DN FGFR4* (Hongo et al. 1999). Artesunate (Sigma, PHR2573) was resuspended in DMSO to make a master stock of 1 M concentration. MG-132 (Sigma, 474790), chloroquine (Sigma, C6628), SU5402 (Sigma, SML0443) and U0126 (Sigma, 662005) were dissolved in DMSO. As a negative control, DMSO was used at a concentration of 0.1%.

### *In situ* hybridization

Whole-mount *in situ* hybridization was performed with digoxigenin (DIG)-labeled probes as described (Harland 1991). Anti-sense RNA *in situ* probes were *in vitro* synthesized using the plasmids containing cDNAs, linearizing restriction enzymes, and SP6, T7 or T3 RNA polymerase as specified: *Goosecoid*, pG500 (BamHI, T3); *Ventx1.2*, pBSK-Ventx1.2 (Sall, T7); *Sox2*, pGEM-T-Sox2 (BamHI, SP6); *E.keratin*, pGEM-T-E.keratin (NcoI, SP6); *Sox9*, pCS2-XSox9 (ClaI, T7); *MyoD*, pGEM-T-MyoD (SpeI, T7); *Otx2*, pBSK-Otx2 (NotI, T7); *HoxB9*, pGEM-T-HoxB9 (SpeI, T7). Hybridization

was detected with an alkaline phosphatase (AP)-conjugated anti-digoxigenin antibody (Roche, 11093274910) and visualized using BM purple as a substrate (Roche, 11442074001). To compare quantitatively the expression levels of marker genes in experimental and control embryos, we selected and measured the areas of expression of markers on photographs by using ImageJ software. In each cases, the results obtained on DMSO or ART-treated embryos were normalized to results obtained on untreated sibling control embryos. During this, the mean value obtained for the untreated control was accepted as a unit.

### Real-time RT-PCR

For each sample, total RNA was isolated from 12 animal cap explants by using TRI Reagent (MRC, TR118) according to the manufacturer's protocols and treated with RNase-free DNase I to eliminate genomic DNA. RNA was reverse transcribed using a random hexamer and M-MLV reverse transcriptase (Promega, M1705) at 37°C for 1 hour. Quantitative real-time PCR was performed using specific primers shown in Supplementary Data 1 and the FastStart Essential DNA Green Master (Roche, 06402712001) on LightCycler 96 system (Roche). The cycling conditions used were: denaturation at 95°C for 10 seconds, annealing at 60°C for 20 seconds, and extension at 72°C for 30 seconds. The real-time PCR results were determined using the Comparative Ct method with ornithine decarboxylase (ODC) as an internal control (data not shown). Each bar on the histograms has been normalized to the level of ODC expression. The histograms in each figure are represented as the mean  $\pm$  SD of three independent experiments.

### Western blot analysis

Animal cap tissues were homogenized in Triton X-100 lysis buffer (50 mM Tris (pH 7.6), 1% Triton X-100, 50 mM NaCl, 1 mM EDTA, 1 mM sodium vanadate, 10 mM NaF, 1 mM PMSF, 20  $\mu$ g/ml aprotinin, 20  $\mu$ g/ml leupeptin). Equal amounts of proteins were separated by 8-10% SDS-PAGE. Western blot analysis was carried out according to standard protocol. Antibodies used for western blot analysis are as follows: anti-Smad1 (1: 4,000; Cell signaling, 6944S), anti-Smad2 (1: 4,000; Cell signaling, 5399S), anti-p-ERK (1: 3,000; Cell signaling, 4377S), anti-ERK (1: 3,000; Cell signaling, 4695S) antibodies.

### Statistical analysis

Experimental data were analyzed by using *t*-test in Microsoft Excel software. A *P* value of less than 0.05 was considered as significant.

## Results

### Morphological deformities in ART-exposed embryos

To observe the effects of ART exposure on the morphology of vertebrate embryos, we started to treat *Xenopus* embryos with incremental doses of ART right after fertilization and reared them in such a condition until untreated sibling embryos developed into tadpoles. While embryos treated with relatively low doses (10-200  $\mu$ M) of ART showed no obvious deformities, exposure to its higher levels (over 500  $\mu$ M) caused a significant proportion of lethality (data not shown). Based on these results, 400  $\mu$ M was selected for the highest concentration in the definitive study. The morphological phenotypes of embryos exposed to ART (400  $\mu$ M) were classified into either 'mild' or 'severe' (Figure 1A). The former includes reduction of body axis, malformation of tail structures and loss of melanophores in the eyes and trunk region of embryos. The severely affected embryos displayed marked truncation of posterior structures, reminiscent of the phenotypes of tadpoles doubly depleted of BMP4/BMP7 (Reversade et al. 2005) or of *Xbra*, an early mesodermal gene (Wu et al. 2022). Given that the melanocytes in the craniofacial region and the lateral and tail pigmentation are neural crest (NC) derivatives, the mild deformities indicate the adverse effects of ART on the ectodermal development in early embryos, including NC formation and neural differentiation. Furthermore, the severe loss of caudal structures suggests its interference with the formation of posterior mesoderm.

Mesodermal specification and ectodermal differentiation occur in a developmental stage-dependent manner. Thus, we sought to determine whether the disruptive effects of ART on the morphology of embryos are time-specific in early development. For this, embryos began to be exposed to ART at distinct time points and were allowed to develop to tadpole stages in the same culture media as shown in Figure 1B. Early exposure to ART from the one-cell stage (stage 1) resulted in the highest proportion of posterior truncation (Figure 1C, I). The mild phenotypes were also seen in some tadpoles with such early exposure to this compound. Relatively late exposure to ART from the mid-blastula (stage 8.5) or early gastrula (stage 10.5) stages was less effective in producing the severe axis deformity than earlier exposure from stage 1. Conversely, the increased proportion of the mild anomalies was observed in the embryos exposed to ART later (II and III). Post-gastrulation treatment with ART exerted marginal effects on the formation of anterior-posterior body axis, though some embryos reared in such a

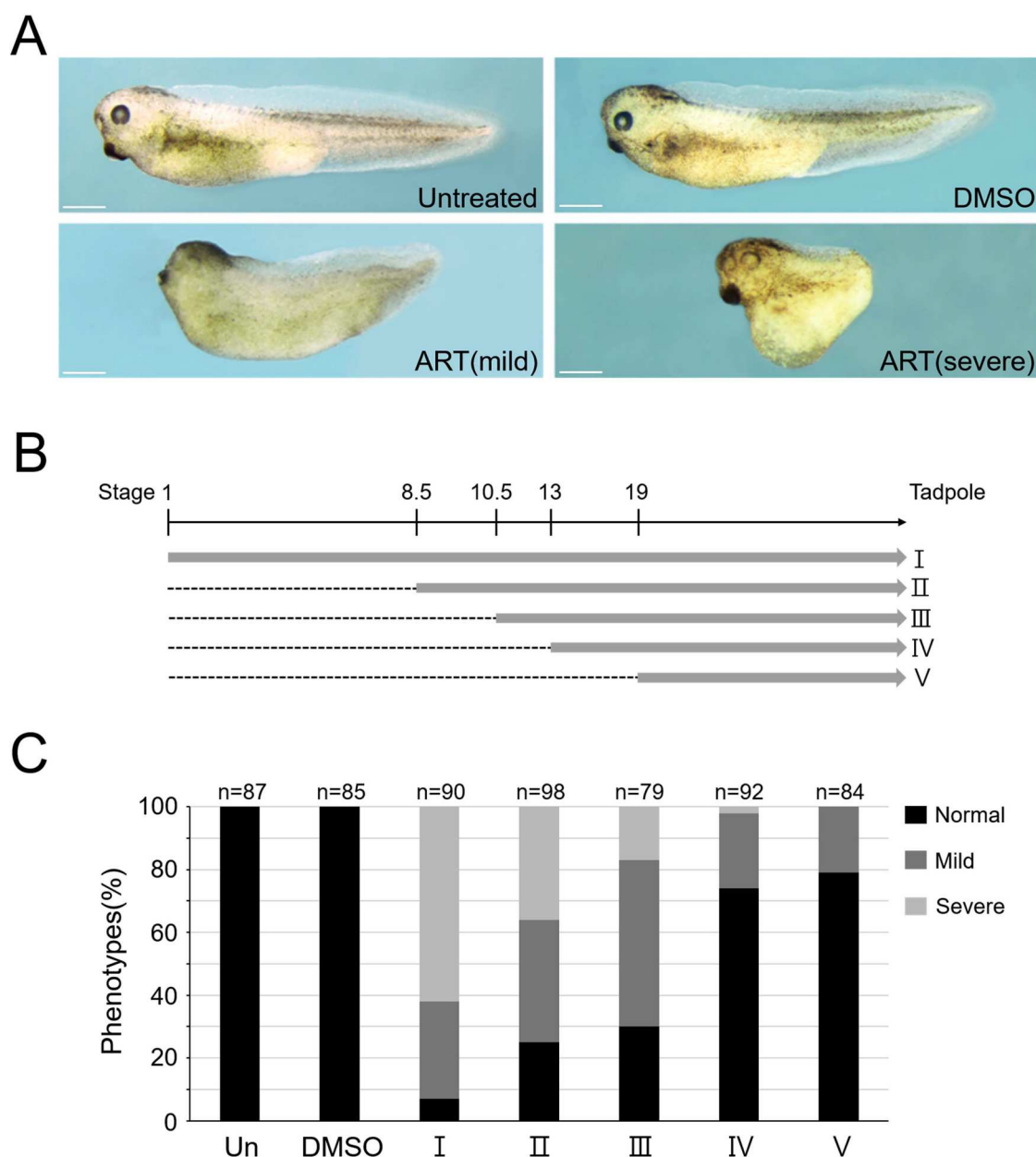


**Figure 1.** Morphological phenotypes of ART-exposed *Xenopus* embryos. (A) Embryos were exposed or not to DMSO (for control) or ART (400  $\mu$ M) from the one-cell stage until the untreated sibling embryos reached tadpole stages. All embryos are shown in lateral views with anterior to the left. Scale bar, 500  $\mu$ m. (B) Experimental design of treatment with ART. Developmental stages are shown from stage 1 to tadpole stage. Embryos were cultured in the presence of ART (400  $\mu$ M) during the periods represented by the gray bars, and the phenotypes were analyzed at the tadpole stage. (C) Quantification of the phenotypes resulting from the treatment conditions shown in (B). DMSO-treated embryos were grown as in (A). Un, untreated control embryo.

condition displayed the mild morphology. Therefore, these results suggest that ART could affect the stability and/or activity of its target at the pre-gastrula and gastrula stages, thereby interfering with the formation of body axis and ectodermal derivatives.

#### ART down-regulates BMP signals

The posteriorly truncated phenotypes of ART-exposed embryos resemble the embryonic anteriorization

generated by knockdown of BMPs, suggesting a possibility of ART acting as an inhibitor of BMP signaling. To ascertain this possibility, we assessed whether ART could down-regulate the expression of target genes induced by BMP signals. For this, animal cap tissues in which the BMP-responsive target genes such as *Ventx2.2* and *Ventx1.2* are expressed, were dissected from the whole embryos, cultured in the presence of ART and analyzed by qPCR. Of note, treatment with ART, but not DMSO, markedly inhibited the transcriptions of those BMP-4 target genes

(Figure 2A, B). In contrast, ART exposure exerted no significant effect on the expression of *Gooseoid* (*Gsc*) induced by Activin, a member of the TGF- $\beta$  superfamily of proteins (Figure 2C). It is well known that when isolated from the embryos, animal cap tissues normally differentiate into epidermis. Inhibition of BMP signaling, however, promotes neural development at the expense of epidermal cell fates in animal cap explants (Wawersik et al. 2005). As shown in Figure 2D, E, ART treatment caused significant down-regulation of the epidermal marker *Epidermal keratin* (*E.keratin*), concomitant with an up-regulation of the pan-neural marker *Sox2*, supporting the inhibitory effects of ART on BMP signaling. Myogenic specification (marked by *MyoD* expression) can be ectopically induced in the ventral marginal zone (VMZ) of embryo by BMP

antagonists alone but not in animal cap tissue (Zetser et al. 2001). This may be because this muscle-specific transcription requires basal mesoderm formation (Osada and Wright 1999), which occurs in the VMZ but not in animal caps. Intriguingly, the expression of *MyoD* was induced in animal cap explants by treatment with ART. Together, these results suggest that ART acts as an inhibitor of BMP signaling, thereby contributing to specification of paraxial mesoderm.

### ART interferes with specification of mesoderm and ectoderm

The above mentioned *in vitro* results prompted us to assess whether ART would interfere with mesodermal

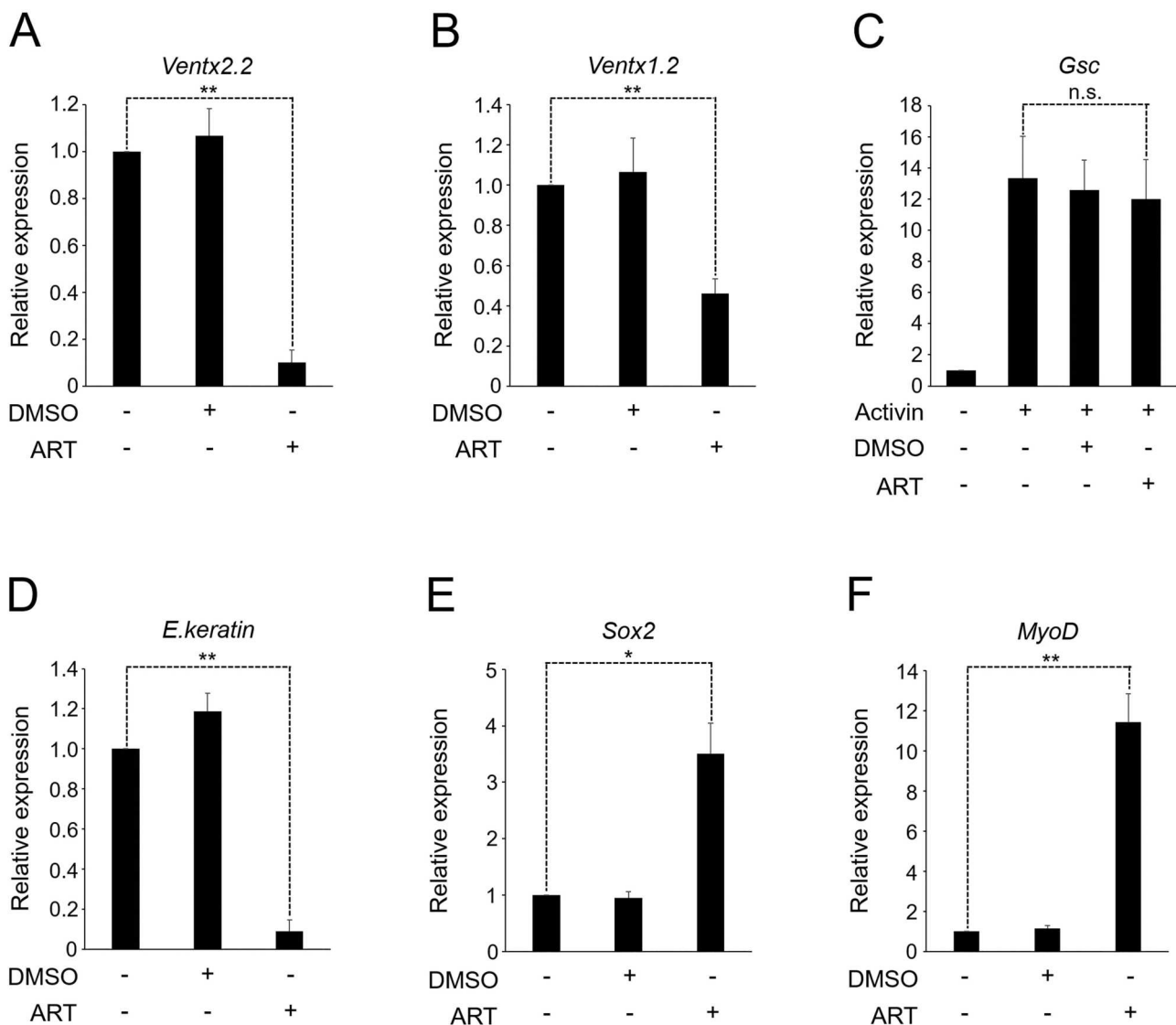


**Figure 2.** ART inhibits BMP signals. (A-F) Animal cap tissues were excised at stage 8.5 from the whole embryos, cultured in the absence or presence of ART (400  $\mu$ M) and/or Activin (2 ng/ml) until the sibling control whole embryos reached stage 10.5 (for *Ventx2.2*, *Ventx1.2* and *Gsc*) or 19 (for *E.keratin*, *Sox2* and *MyoD*) and then harvested for qPCR experiments. \* $P < 0.05$ , \*\* $P < 0.01$  by unpaired Student's *t*-test. n.s., not significant.



and ectodermal differentiation *in vivo* which are regulated by BMP signaling. To this end, *in situ* hybridization experiments were conducted to examine changes in the expression patterns of key markers in ART-treated embryos. Notably, treatment with ART abrogated the expression of *Ventx1.2* in the ventral and ventrolateral marginal zone of gastrulae (Figure 3A), suggesting its inhibitory effects on the specification of ventral mesoderm by BMP signals. However, the expression of *Gsc* in the organizer of early gastrula embryo was not altered by exposure to ART. Thus, these results indicate the specific negative effects of ART on the BMP-dependent specification of mesoderm.

ART exposure also caused the lateral expansion of *Sox2* expression into the presumptive epidermal territory, compared to that in untreated or DMSO-treated control embryos (Figure 3B). By contrast, epidermal tissue was significantly reduced in ART-exposed embryos as evidenced by the abrogated expression of

*E.keratin* in the dorsolateral region. Furthermore, the expression of the neural crest (NC) marker *Sox9* was shifted laterally and decreased by exposure to ART, compared to that in control embryos. Anti-BMP and FGF signals have similar effects on ectodermal differentiation, enhancing neural development at the expense of epidermal cell fates (Pera et al. 2003). However, neural fate induced by BMP inhibitors is of anterior character, whereas FGF signals induce posterior type of neural tissue (Ribisi et al. 2000). To further characterize the neural-promoting activity of ART, we next investigated its effects on the anterior-posterior neural patterning. As shown in Figure 3C, the expression of the forebrain/midbrain marker *Otx2* was expanded by exposure to ART, compared to that in control embryos. Expression of the spinal cord marker *HoxB9*, however, appeared normal in ART-treated embryos. These effects of ART indicate its role as an inhibitor of BMP signals. In line with this, *MyoD* expression was laterally

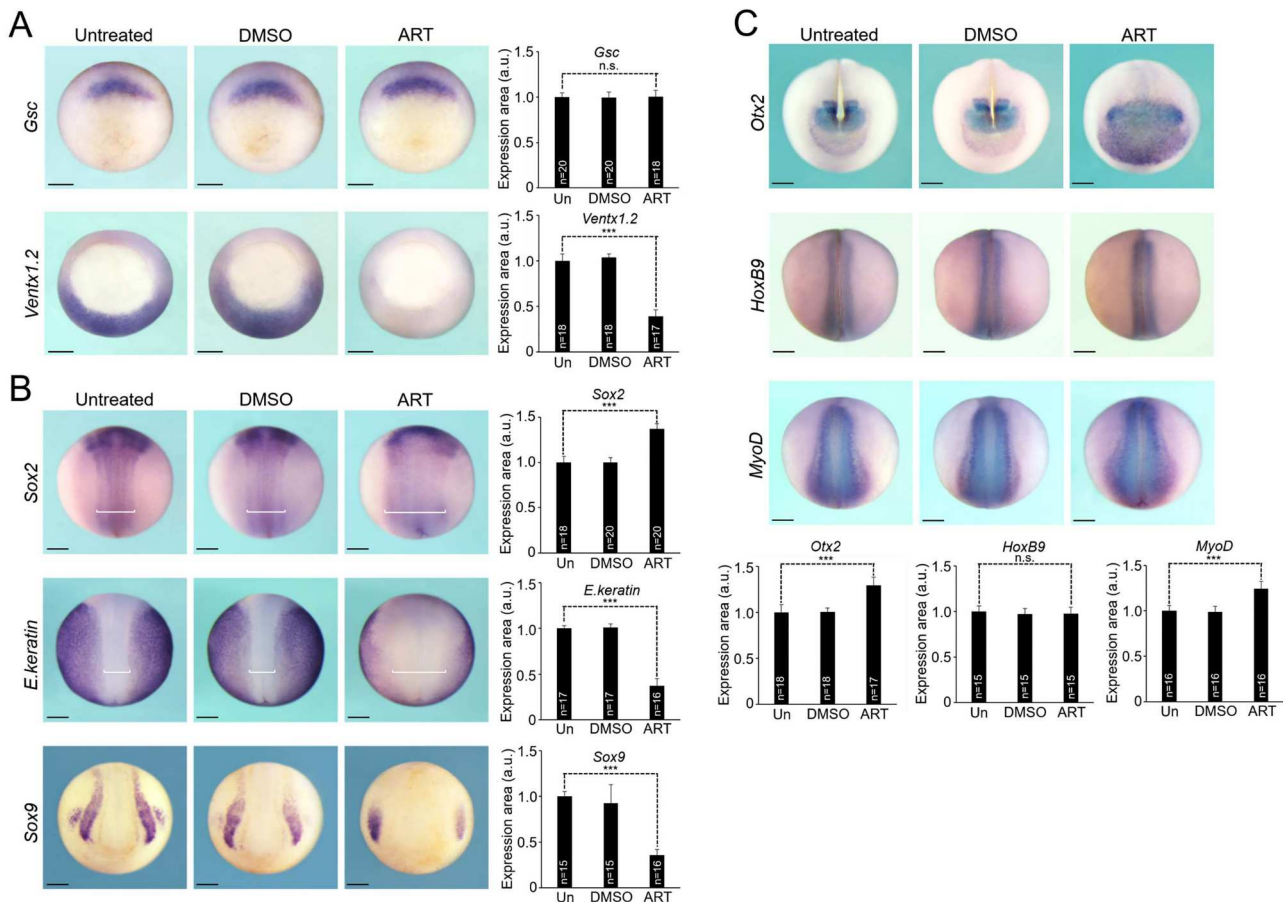


**Figure 3.** Interfering effects of ART on germ layer specification. (A–C) Embryos were treated or not with DMSO or ART (400  $\mu$ M) as indicated from stage 8.5 until the untreated sibling embryos reached stage 10.5 (for *Gsc* and *Ventx1.2*), 16 (for *Sox2*, *E.keratin* and *Sox9*) or 19 (for *Otx2*, *HoxB9* and *MyoD*) and then subjected to *in situ* hybridization against these markers. Embryos are shown in vegetal view with dorsal to the top (panels in (A)), in dorsal view with anterior to the top (panels in upper two tiers in (B) and panels in lower two tiers in (C)) or in anterior view with dorsal to the top (panels in bottom tier in (B) and panels in top tier in (C)). Scale bar, 250  $\mu$ m. The histograms in each figure are presented as the mean  $\pm$  SD (n, number of analyzed embryos). \*\*\* $P$  < 0.001 by unpaired Student's *t*-test. n.s., not significant. Un, untreated control embryo.

expanded in the posterior region of embryo upon exposure to ART, which is similar to that in BMP-depleted embryos (Reversade et al. 2005), indicating an expansion of paraxial tissue into ventroposterior mesoderm. Overall, these results suggest that ART interferes with BMP signaling to promote neural differentiation at the expense of epidermal and NC cell fates.

### ART induces degradation of Smad1

We next sought to investigate the underlying mechanisms by which ART impedes BMP signaling. For this, we analyzed the effects of ART on the cellular levels of

key signaling molecules in animal cap tissue. Intriguingly, the naïve ectodermal cells treated with ART displayed an increased level of phospho-p44/42 MAPK (ERK1/2) (Figure 4A), indicative of its up-regulation of MAP kinase activity. It is also of note that the cellular level of Smad1, a downstream mediator of BMP signaling was down-regulated by exposure to ART. In contrast, the level of Smad2, which mediates Activin/Nodal signaling, remained unchanged in ART-treated animal cap cells. These results suggest that ART exposure induces degradation of Smad1, leading to inhibition of BMP signaling. Thus, we further assessed the effect of ART on the steady state level of Smad1. As depicted in Figure 4B,

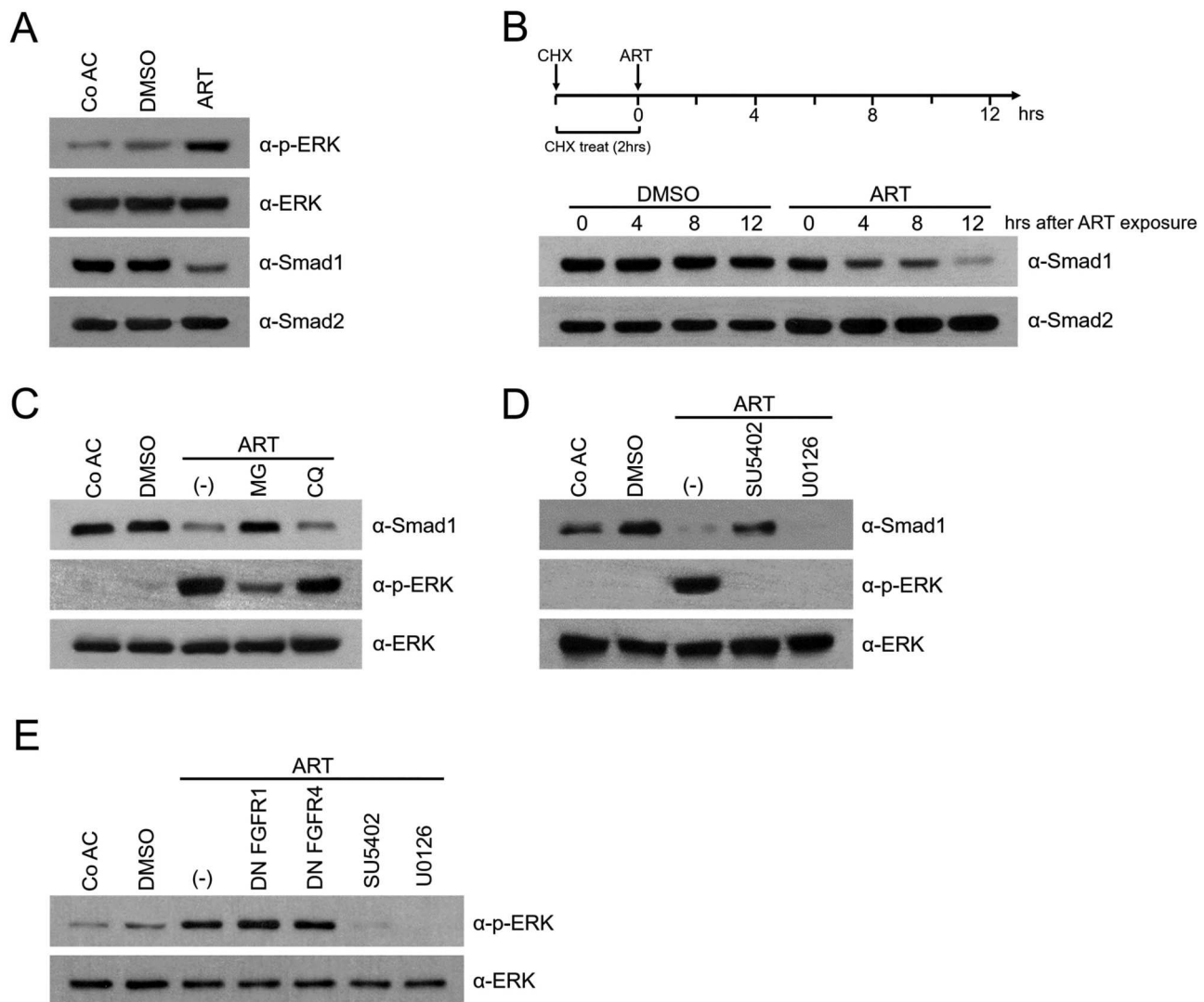


**Figure 4.** ART induces ERK activation via Smad1 turnover. (A) Animal caps excised at stage 8.5 from the whole embryos were cultured to stage 12 in the presence or absence of ART (400  $\mu$ M) and then subjected to western blotting. (B) Embryos were pre-treated with cycloheximide (CHX, 10  $\mu$ g/ml) for 2 hours before animal cap explants were excised at stage 8.5 from the whole embryos. Dissected animal cap cells were exposed to DMSO or ART for the indicated times and then harvested for western blot analysis. (C-E) Four-cell stage embryos were injected or not in the animal pole region with *DN FGFR1* (500 pg) or *DN FGFR4* (500 pg) mRNA as indicated, and then animal cap tissues were dissected at stage 8.5, cultured in media containing DMSO or ART with or without MG-132 (MG, 10  $\mu$ M), chloroquine (CQ, 100  $\mu$ M), SU5402 (20  $\mu$ M) or U0126 (20  $\mu$ M) as denoted and harvested at stage 12 for western blotting. Co AC, untreated control animal cap. (-) in (C-E) indicates animal caps treated with ART only.

after pre-treatment with the protein synthesis inhibitor cycloheximide, animal cap cells were exposed to ART for specific times to observe the profile of Smad1 degradation. This analysis revealed that the turnover of Smad1 is accelerated by ART exposure, compared to that in DMSO-treated control cells. Furthermore, this ART-induced degradation of Smad1 was attenuated by co-treatment with the proteasome inhibitor MG-132 (MG), but not by the lysosomal inhibitor chloroquine (CQ) (Figure 4C). These results suggest that ART promotes the degradation of Smad1 in a proteasome-dependent manner.

FGF signal has been shown to induce the MAPK-mediated linker phosphorylation and subsequent proteasomal degradation of Smad1, thereby promoting neural differentiation (Pera et al. 2003). Given that ART exposure led to ERK activation and expansion of the neural plate as shown above, it is possible that ART induces ERK activation, resulting in the linker phosphorylation and turnover of Smad1. Notably, treatment with MG-132 reversed both ERK phosphorylation and Smad1 degradation induced by ART exposure (Figure 4C). Chloroquine, however, had no effects on these ART-induced events. These results indicate that ART promotes the degradation of Smad1, thereby leading to ERK phosphorylation, but not vice versa. In support of this, the ART-induced turnover of Smad1 occurred even in the presence of the MAPK kinase (MEK) inhibitor U0126 (Figure 4D). It is of interest that co-treatment with the FGF receptor (FGFR) inhibitor SU5402 could suppress the degradation of Smad1 as well as ERK phosphorylation which is induced by ART exposure. Together, these data suggest that the downstream signaling events of FGFR, but not ERK activation, may be necessary for ART induction of Smad1 degradation.

Several studies have reported that inhibition of BMP signaling leads to upregulation of MAPK activity (Goswami et al. 2001; Cho et al. 2013). BMP4 signaling inhibits ERK activity via induction of dual-specificity phosphatase 9 (DUSP9), an ERK-specific phosphatase in determination of embryonic stem cell fate (Li et al. 2012). Given these findings, it is possible that ART inhibition of BMP signaling abrogates induction of a negative regulator targeting ERK, thereby leading to upregulation of ERK activity. As shown in Figure 4E, ART promotion of ERK phosphorylation did not occur in SU5402 or U0126-treated animal cap cells. This may be due to the complete absence of ERK phosphorylation caused by these inhibitors, though ART attenuates induction of a regulator interfering with ERK phosphorylation. Several types of FGFRs, including FGFR1, 2, 3, 4a and 4b, are expressed in the gastrula ectodermal cells

(Hongo et al. 1999), and the most common pathway initiated by FGFs is the MAPK pathway (Bottcher and Niehrs 2005). Thus, expression of respective dominant-negative (DN) mutants of these FGFRs would partially reduce ERK phosphorylation in animal cap cells as opposed to the general FGFR inhibitor SU5402. Next, we wanted to check whether ART enhancement of ERK phosphorylation would be seen in animal cap cells expressing a DN FGFR mutant. Of note, inhibition of FGFR1 or FGFR4 activity by expression of their respective DN mutants exerted no effects on ART induction of an increase in the levels of phosphorylated ERK (Figure 4E). Overall, these results suggest that ART may abrogate via induction of Smad1 turnover the BMP-dependent expression of an ERK-specific inhibitory regulator.

## Discussion

In *Xenopus* early development, BMP signals play key roles in establishing the dorsoventral (DV) pattern of germ layers. Embryos triply depleted of BMP2, BMP4 and BMP7 displayed compromised trunk and tail development (Reversade et al. 2005), indicative of loss of ventral and posterior mesodermal cell fates. BMP antagonists emanating from the organizer block BMP signaling *in vivo*, inducing neural differentiation at the expense of epidermal fate. In this work, ART-treated tadpoles showed severe truncation of posterior structures, reminiscent of the phenotypes of embryo lacking BMPs. ART exposure also caused expansion of the neural plate concomitant with a reduction of epidermal territory. These adverse effects of ART on embryonic development suggest its role as an inhibitor of BMP signaling pathway. In support of this, transcriptions of BMP-responsive target genes were attenuated in the ectoderm and mesoderm of ART-exposed embryos. In addition, ART treatment led to laterally expanded expression of the myogenic factor MyoD in the posterior region of embryo, which was also observed in BMPs-depleted embryos. Inhibition of BMP signaling at the blastula stages causes a dramatic increase in anterior neural tissues as marked by *Otx2*, whereas expression of this forebrain marker is reduced when late BMP signaling is inhibited at the gastrula stages (Cho et al. 2013). Thus, the expanded expression of *Otx2* in ART-treated embryos suggests the inhibitory effects of this compound on early BMP signaling in the blastulae. Unexpectedly, we found that ART facilitates the degradation of Smad1, a key mediator of BMP signaling in a proteasome-dependent manner. This action could be an underlying mechanism by which ART interferes with BMP signaling pathway. Collectively, these results suggest that ART exerts



severe teratogenic effects on the specification of germ layers by impeding BMP signaling in vertebrate early development.

ART induction of Smad1 degradation led to an increase in the levels of phosphorylated ERK (Figure 4), indicative of the inhibitory effects of BMPs on MAPK activity. In some developmental processes, BMP signaling down-regulates MAPK activity. BMP-4 blocks MAPK activity via a TAK1/p38-type pathway in *Xenopus* ectoderm for the repression of neural cell fate (Goswami et al. 2001). This inhibition is independent of de novo protein synthesis, presumably involving the p38-type kinase-mediated activation of MAPK-specific phosphatase. Late BMP signaling after mid-gastrulation is essential for anterior neural specification in *Xenopus* early embryo (Cho et al. 2013). In the formation of anterior neural tissues, BMP induction of a transcriptional repressor Tbx2 leads to suppression of the expression of Flrt3, a positive regulator of FGF signaling (Cho et al. 2017). As a result of this regulatory cascade, BMP signaling interferes with FGF-induced ERK phosphorylation and caudalization of neural fate. BMP-4 also inhibits ERK activity in sustaining the self-renewal status of mouse embryonic stem cells (ESCs) (Li et al. 2012). For this control, BMP-4 induces the expression of ERK-specific phosphatase DUSP9, which is mediated by Smad1 and Smad4. It appears that ART disrupts early BMP signaling at the pre-gastrula stages as evidenced by the expansion of anterior neural fate in ART-exposed embryo. Thus, ART upregulation of ERK activity is unlikely to occur due to inhibition of the BMP/Tbx2 pathway. Since the BMP/TAK1 pathway inhibits MAPK activity independently of Smad1 function, ART seems not to interfere with this pathway to upregulate MAPK activity. ART-induced Smad1 degradation was necessary for its enhancement of ERK activity (Figure 4C), suggesting the possibility that Smad1-mediated induction of an ERK-specific inhibitory regulator may be impaired in ART-exposed cells. FGFs are thought to be major activators of MAPK in *Xenopus* early development (Christen and Slack 1999). Thus, the marginal zone of the embryo in which expression of different FGFs is enriched, has high MAPK activity, whereas relatively lower activity of MAPK is present in the animal pole (LaBonne et al. 1995). Given the negative effects of BMPs on MAPK activity, high BMP activity in the animal pole might also contribute to maintaining the low levels of MAPK activity in this region of the embryo. Notably, ART induction of Smad1 turnover, which disrupts BMP signals, resulted in a marked increase in the levels of ERK activity in the animal cap cells. This indicates that an ERK-specific negative regulator whose expression is blocked by ART exposure, plays predominant roles in sustaining low

MAPK activity in the animal pole of the embryo. Nevertheless, ART abrogation of Smad1 function caused no increased activity of ERK when ERK activation was totally impeded by treatment with SU5402 or U0126 (Figure 4E). Further studies are necessary to identify the ERK-specific negative regulator and molecular mechanism by which this ERK-targeting regulator and MAPK kinase (MEK) modulate the equilibrium between phosphorylation and dephosphorylation of ERK.

Inhibition of BMP signaling in the ventral marginal zone (VMZ) of embryo alters its fate to a more dorsal type of mesoderm, thereby causing its differentiation into skeletal muscle (marked by *MyoD* expression) (Zetser et al. 2001). This BMP antagonism in the VMZ also induces upregulation of MAPK activity, which is required for myogenic specification to ensue. By contrast, ectopic expression of *MyoD* cannot be induced by a BMP antagonist alone in the animal cap cells, though MAPK activity is still increased by this block of BMP signaling (Uzgare et al. 1998). Myogenic specification occurs in the animal cap cells stimulated with FGF or Activin/Nodal signals (Osada and Wright 1999), suggesting that basal mesoderm induction and anti-BMP signal are essential for activation of muscle determination. This may be the reason that BMP antagonism alone can induce myogenic differentiation in the VMZ, from which the ventral mesoderm emerges. In this respect, it is noticeable that ART can induce the ectopic expression of *MyoD* in the animal cap cells. Possibly, the enhanced ERK activity and/or other signaling events induced by ART exposure may contribute to basal mesoderm formation, which merits further investigation. Constitutive FGF signal in ectoderm is required for BMP antagonists to induce anterior neural specification in this naïve tissue (Hongo et al. 1999). Overexpression of a MAPK-specific phosphatase in ectoderm inhibits MAPK activity and prevents neural differentiation in response to inducing signals from the organizer (Uzgare et al. 1998). These findings suggest that a certain level of MAPK activity is critical for BMP inhibition-induced neural development in ectoderm. Nonetheless, inhibition of BMP signaling alone induces neural tissue through a default pathway in *Xenopus* ectoderm (De Robertis and Kuroda 2004). As shown in our results, ART exposure alone caused neuralization in the animal cap cells. Thus, we postulate that ERK activity upregulated by ART or BMP inhibitors might play significant roles in inducing neural cell fate.

ART has been shown to induce proteasome-dependent degradation of specific signaling molecules in cancer cells. ART promotes anti-tumor immunity by reducing the levels of the transcriptional coactivator

of the Hippo pathway, TAZ in lung cancer cells (Cao et al. 2022; Jang et al. 2023). However, the exact mechanism underlying ART-induction of proteasomal degradation of TAZ remains unknown. KRAS acts as a molecular switch downstream of EGF receptor and its mutation is one of the dominant mutations in colorectal cancer (CRC). ART enhances KRAS degradation in a proteasome-dependent manner to inhibit CRC growth, which involves increasing the levels of E3 ligase ANAPC2 and  $\beta$ -TrCP and the expression of GSK3- $\beta$  (Gong et al. 2022). As shown in our work, ART also accelerates the proteasomal turnover of Smad1, which is inhibited by treatment with SU5402 but not by U0126. This suggests that signaling events downstream of FGFR, but not ERK activation, plays essential roles in ART induction of Smad1 degradation. Signaling pathways activated through FGFRs include the Ras/MAPK, PI3 kinase/Akt and PLC $\gamma$ /Ca<sup>2+</sup> pathways (Bottcher and Niehrs 2005). Given that the ubiquitin-proteasome system is regulated by Akt activity or intracellular calcium level (Yazaki et al. 2012; Xu et al. 2015), it is tempting to speculate that ART induction of proteasomal degradation of Smad1 might be controlled by the PI3 kinase/Akt and/or PLC $\gamma$ /Ca<sup>2+</sup> pathways. Reactive oxygen species (ROS) elicited by ART has been shown to play a key role in ART-induced apoptosis in different tumor cell types as well as its anti-malarial activity. Notably, ROS are involved in the activation of several serine/threonine kinases, including ERK, JNKs and PKC (Lefaki et al. 2017). PKC is an important kinase that alters the expression of various genes upon oxidative stress. In addition, the activities of several transcription factors such as NF- $\kappa$ B, p53, FOXO, and AP-1 are modulated in response to oxidative stress. Thus, it is possible that ART generation of ROS leads to gene responses via activation of PKC or transcriptional factors, which may be critical for ART induction of Smad1 degradation. Since the PLC $\gamma$ /Ca<sup>2+</sup> pathway is also responsible for the activation of PKC (Bottcher and Niehrs 2005), this signaling cascade triggered by FGFs might be necessary for ROS-mediated activation of PKC. Future experiments are warranted to investigate in detail the mechanism by which ART causes Smad1 turnover and its association with FGF signaling pathways.

### Ethical approval statement

This study was conducted in accordance with all relevant ethical regulations regarding animal research. All animal experiments were approved by the Institutional Animal Care and Use Committee at the Asan Institute for Life Sciences, Asan Medical Center

### Acknowledgement

Kim M.S. and Yoon G-H. designed and performed the experiments. All authors analyzed and discussed the data. Choi S-C. conceived the study and supervised the project. Choi S-C. wrote the manuscript.

### Disclosure statement

The authors declare that they have no known competing financial interests or personal relationships that could have appeared to influence the work reported in this paper.

### Funding

This work was supported by the National Research Foundation of Korea (NRF) grant funded by the Korea government (MSIT) (2022R1A2C1011769).

### ORCID

Myeoung Su Kim  <http://orcid.org/0009-0000-1874-3484>  
Gang-Ho Yoon  <http://orcid.org/0009-0002-6755-6225>  
Sun-Cheol Choi  <http://orcid.org/0000-0003-3366-894X>

### References

- Bottcher RT, Niehrs C. 2005. Fibroblast growth factor signaling during early vertebrate development. *Endocr Rev.* 26:63–77.
- Cao D, Chen D, Xia JN, Wang WY, Zhu GY, Chen LW, Zhang C, Tan B, Li H, Li YW. 2022. Artesunate promoted anti-tumor immunity and overcame EGFR-TKI resistance in non-small-cell lung cancer by enhancing oncogenic TAZ degradation. *Biomed Pharmacother.* 155:113705.
- Chen Y, Wang F, Wu P, Gong S, Gao J, Tao H, Shen Q, Wang S, Zhou Z, Jia Y. 2021. Artesunate induces apoptosis, autophagy and ferroptosis in diffuse large B cell lymphoma cells by impairing STAT3 signaling. *Cell Signal.* 88:110167.
- Cho GS, Choi SC, Han JK. 2013. BMP signal attenuates FGF pathway in anteroposterior neural patterning. *Biochem Biophys Res Commun.* 434:509–515.
- Cho GS, Park DS, Choi SC, Han JK. 2017. Tbx2 regulates anterior neural specification by repressing FGF signaling pathway. *Dev Biol.* 421:183–193.
- Christen B, Slack JM. 1999. Spatial response to fibroblast growth factor signalling in *Xenopus* embryos. *Development.* 126:119–125.
- De Robertis EM, Kuroda H. 2004. Dorsal-ventral patterning and neural induction in *Xenopus* embryos. *Annu Rev Cell Dev Biol.* 20:285–308.
- De Robertis EM, Larrain J, Oelgeschlager M, Wessely O. 2000. The establishment of Spemann's organizer and patterning of the vertebrate embryo. *Nat Rev Genet.* 1:171–181.
- Fuentealba LC, Eivers E, Ikeda A, Hurtado C, Kuroda H, Pera EM, De Robertis EM. 2007. Integrating patterning signals: Wnt/GSK3 regulates the duration of the BMP/Smad1 signal. *Cell.* 131:980–993.
- Gong RH, Chen M, Huang C, Wong HLX, Kwan HY, Bian Z. 2022. Combination of artesunate and WNT974 induces KRAS protein degradation by upregulating E3 ligase ANAPC2

- and beta-TrCP in the ubiquitin-proteasome pathway. *Cell Commun Signal.* 20:34.
- Goswami M, Uzgaré AR, Sater AK. 2001. Regulation of MAP kinase by the BMP-4/TAK1 pathway in *Xenopus* ectoderm. *Dev Biol.* 236:259–270.
- Goutam RS, Kumar V, Lee U, Kim J. 2024. Cdx1 and Gsc distinctly regulate the transcription of BMP4 target gene *ventx3.2* by directly binding to the proximal promoter region in *Xenopus* gastrulae. *Mol Cells.* 47:100058.
- Harland RM. 1991. In situ hybridization: an improved whole-mount method for *Xenopus* embryos. *Methods Cell Biol.* 36:685–695.
- Hogan BL. 1996. Bone morphogenetic proteins: multifunctional regulators of vertebrate development. *Genes Dev.* 10:1580–1594.
- Hongo I, Kengaku M, Okamoto H. 1999. FGF signaling and the anterior neural induction in *Xenopus*. *Dev Biol.* 216:561–581.
- Jang W, Im M, Roh J, Kang J, Kim W. 2023. Hippo-YAP/TAZ pathway regulation: the crucial roles of lncRNAs in cancer. *Anim Cells Syst (Seoul).* 27:309–320.
- Kim SJ, Park SH, Myung K, Lee KY. 2024. Lamin A/C facilitates DNA damage response by modulating ATM signaling and homologous recombination pathways. *Anim Cells Syst (Seoul).* 28:401–416.
- Kumar S, Umair Z, Kumar V, Goutam RS, Park S, Lee U, Kim J. 2024. Xbra modulates the activity of linker region phosphorylated Smad1 during *Xenopus* development. *Sci Rep.* 14:8922.
- LaBonne C, Burke B, Whitman M. 1995. Role of MAP kinase in mesoderm induction and axial patterning during *Xenopus* development. *Development.* 121:1475–1486.
- Lefaki M, Papaevgeniou N, Chondrogianni N. 2017. Redox regulation of proteasome function. *Redox Biol.* 13:452–458.
- Li Z, Fei T, Zhang J, Zhu G, Wang L, Lu D, Chi X, Teng Y, Hou N, Yang X, et al. 2012. BMP4 signaling acts via dual-specificity phosphatase 9 to control ERK activity in mouse embryonic stem cells. *Cell Stem Cell.* 10:171–182.
- Moustakas A, Heldin CH. 2009. The regulation of TGFbeta signal transduction. *Development.* 136:3699–3714.
- Niehrs C. 2004. Regionally specific induction by the Spemann-Mangold organizer. *Nat Rev Genet.* 5:425–434.
- Osada SI, Wright CV. 1999. *Xenopus* nodal-related signaling is essential for mesendodermal patterning during early embryogenesis. *Development.* 126:3229–3240.
- Park DS, Yoon GH, Lee HS, Choi SC. 2016. Capsaicin inhibits the Wnt/beta-catenin signaling pathway by down-regulating PP2A. *Biochem Biophys Res Commun.* 478:455–461.
- Pera EM, Ikeda A, Eivers E, De Robertis EM. 2003. Integration of IGF, FGF, and anti-BMP signals via Smad1 phosphorylation in neural induction. *Genes Dev.* 17:3023–3028.
- Reversade B, Kuroda H, Lee H, Mays A, De Robertis EM. 2005. Depletion of Bmp2, Bmp4, Bmp7 and Spemann organizer signals induces massive brain formation in *Xenopus* embryos. *Development.* 132:3381–3392.
- Ribisi S, Jr., Mariani FV, Aamar E, Lamb TM, Frank D, Harland RM. 2000. Ras-mediated FGF signaling is required for the formation of posterior but not anterior neural tissue in *Xenopus laevis*. *Dev Biol.* 227:183–196.
- Sapkota G, Alarcon C, Spagnoli FM, Brivanlou AH, Massague J. 2007. Balancing BMP signaling through integrated inputs into the Smad1 linker. *Mol Cell.* 25:441–454.
- Uzgaré AR, Uzman JA, El-Hodiri HM, Sater AK. 1998. Mitogen-activated protein kinase and neural specification in *Xenopus*. *Proc Natl Acad Sci U S A.* 95:14833–14838.
- Wawersik S, Evola C, Whitman M. 2005. Conditional BMP inhibition in *Xenopus* reveals stage-specific roles for BMPs in neural and neural crest induction. *Dev Biol.* 277:425–442.
- Wu MY, Hill CS. 2009. Tgf-beta superfamily signaling in embryonic development and homeostasis. *Dev Cell.* 16:329–343.
- Wu Y, Devotta A, Jose-Edwards DS, Kugler JE, Negron-Pineiro LJ, Braslavskaya K, Addy J, Saint-Jeannet JP, Di Gregorio A. 2022. Xbp1 and Brachyury establish an evolutionarily conserved subcircuit of the notochord gene regulatory network. *Elife.* 11:e73992.
- Xu D, Shan B, Lee BH, Zhu K, Zhang T, Sun H, Liu M, Shi L, Liang W, Qian L, et al. 2015. Phosphorylation and activation of ubiquitin-specific protease-14 by Akt regulates the ubiquitin-proteasome system. *Elife.* 4:e10510.
- Yang X, Zheng Y, Liu L, Huang J, Wang F, Zhang J. 2021. Progress on the study of the anticancer effects of artesunate. *Oncol Lett.* 22:750.
- Yazaki M, Kashiwagi K, Aritake K, Urade Y, Fujimori K. 2012. Rapid degradation of cyclooxygenase-1 and hematopoietic prostaglandin D synthase through ubiquitin-proteasome system in response to intracellular calcium level. *Mol Biol Cell.* 23:12–21.
- Zahn N, James-Zorn C, Ponferrada VG, Adams DS, Grzymkowski J, Buchholz DR, Nascone-Yoder NM, Horb M, Moody SA, Vize PD, Zorn AM. 2022. Normal Table of *Xenopus* development: a new graphical resource. *Development.* 149(14):dev200356.
- Zetser A, Frank D, Bengal E. 2001. MAP kinase converts MyoD into an instructive muscle differentiation factor in *Xenopus*. *Dev Biol.* 240:168–181.
- Zhao GQ. 2003. Consequences of knocking out BMP signaling in the mouse. *Genesis.* 35:43–56.